Influence of Resolution in Irrigated Area Mapping and Area Estimation

N.M. Velpuri, P.S. Thenkabail, M.K. Gumma, C. Biradar, V. Dheeravath, P. Noojipady, and L. Yuanjie

Abstract

The overarching goal of this paper was to determine how irrigated areas change with resolution (or scale) of imagery. Specific objectives investigated were to (a) map irrigated areas using four distinct spatial resolutions (or scales), (b) determine how irrigated areas change with resolutions, and (c) establish the causes of differences in resolution-based irrigated areas. The study was conducted in the very large Krishna River basin (India), which has a high degree of formal contiguous, and informal fragmented irrigated areas. The irrigated areas were mapped using satellite sensor data at four distinct resolutions: (a) NOAA AVHRR Pathfinder 10,000 m, (b) Terra MODIS 500 m, (c) Terra MODIS 250 m, and (d) Landsat ETM+ 30 m. The proportion of irrigated areas relative to Landsat 30 m derived irrigated areas (9.36 million hectares for the Krishna basin) were (a) 95 percent using MODIS 250 m, (b) 93 percent using MODIS 500 m, and (c) 86 percent using AVHRR 10,000 m. In this study, it was found that the precise location of the irrigated areas were better established using finer spatial resolution data. A strong relationship (R^2 = 0.74 to 0.95) was observed between irrigated areas determined using various resolutions. This study proved the hypotheses that "the finer the spatial resolution of the sensor used, greater was the irrigated area derived," since at finer spatial resolutions, fragmented areas are detected better. Accuracies and errors were established consistently for three classes (surface water irrigated, ground water/conjunctive use irrigated, and non-irrigated) across the four resolutions mentioned above. The results showed that the Landsat data provided significantly higher overall accuracies (84 percent) when compared to MODIS 500 m (77 percent), MODIS 250 m (79 percent), and AVHRR 10,000 m (63 percent).

N.M. Velpuri is with Geographic Information Science, Center of Excellence, South Dakota State University, 1021 Medary Ave, Wecota Hall, Box 506B, Brookings, SD 57007 (Manohar.Velpuri@sdstate.edu).

P.S. Thenkabail is with the Southwest Geographic Science Center, U.S. Geological Survey (USGS), Flagstaff, Arizona.

M.K. Gumma is with the International Water Management Institute, Hyderabad, India.

C. Biradar is with the Center for Spatial Analysis, University of Oklahoma, Norman, Oklahoma.

V. Dheeravath is with the United Nations Joint Logistics Center-WFP, Juba, Sudan.

P. Noojipady, and L. Yuanjie are with the Department of Geography, University of Maryland, College Park, Maryland.

All the authors were formerly with International Water Management Institute, Colombo, Sri Lanka.

Introduction

Water and food are the two basic human needs. Water in the form of rain or irrigation is necessary to produce food. Of all water available on this globe only 3 percent is freshwater. Out of this, only 1 percent is available for human use. Though, on average, we have sufficient water to meet human needs, the problem we face is its distribution. The occurrence of floods in one region and droughts in the adjacent region has become a common phenomenon. Such problems are resolved to some extent by means of established irrigation systems. The amount of area under irrigation has gradually increased over years in most countries (see Thenkabail *et al.*, 2006, 2009a, and 2009b; **http://www.iwmigiam.org/**). With the water available for human use, the irrigation sector is the highest consumer of water (70 to 80 percent). One of the most important issues in the world food policy debate is whether additional demand will require large investments in additional irrigation systems or whether increased yields and productivity from rain-fed agriculture can satisfy the growing demand for food (see Molden *et al.*, 2007). This issue has become increasingly important as water in developing countries is becoming increasingly scarce and water development increasingly expensive, and in some cases, environmentally destructive (Droogers, 2002). In the current context of water scarcity, it becomes even more important to exactly compute the water available for irrigation and to estimate the efficiency of water use by quantifying the irrigated areas and their production.

Conventional methods of mapping irrigated areas through surveys are time-consuming and tedious. Remote sensing offers a relatively inexpensive and reliable technology to estimate area under irrigation (Thenkabail *et al.*, 2006). Satellites in space have the capacity to continuously monitor the earth, and hence this technology is better used not only for continuous monitoring of irrigation but also for reporting the changes that occur over time for the management of water resources. There are several methods not only of mapping and reporting areas under irrigation using statistics and geospatial techniques (Siebert *et al.*, 2006) and satellite sensor data (Thenkabail *et al.*, 2006, 2009a, and 2009b) but for producing maps at various scales and resolutions. But the knowledge and understanding on the effect of the use of different satellite products with different resolutions on the final accuracies of each map produced are limited.

Photogrammetric Engineering & Remote Sensing
Vol. 75, No. 12, December 2009, pp. 1383–1395.

0099-1112/09/7512–1383/$3.00/0

Background and Rationale

A number of studies have been conducted using advanced tools to monitor irrigated agriculture (Thiruvengadachari and Sakthivadivel, 1997; Bastiaanssen *et al.*, 1999; Shakthivadivel *et al.*, 1999; Ambast *et al.*, 2002; Ozdogan, 2003). These studies primarily used high-spatial-resolution satellite data sets such as Landsat and Indian Remote Sensing Linear Self-Imaging Scanner (IRS LISS) for irrigated area mapping over smaller areas. Draeger (1977) demonstrated the utility of Landsat imagery for fast and cheap estimation of irrigated land area in the Klamath River basin of Oregon. Keene and Conley (1980) used video image analysis techniques to map irrigated areas in Kansas. Thiruvengadachari (1981) used Landsat data to identify irrigation patterns in semiarid areas in India. Rundquist *et al.* (1989) used Landsat data to make an inventory of central pivot irrigation systems in Nebraska. Abderrahman and Bader (1992) mapped the irrigated areas of the severely arid regions of Saudi Arabia using multitemporal Landsat Multispectral Scanner and Thematic Mapper data. Murthy *et al.* (1998) used IRS LISS data to derive a cropping calendar for a canal operation schedule in India. Nevertheless, using high-spatial-resolution data over larger areas, especially in global studies, is highly resource-intensive. Furthermore, such studies using time series are resource-intensive at the global level.

However, Thenkabail *et al.* (2006, 2009a, and 2009b) demonstrated that mapping irrigated areas over the entire world, using time-series coarse-resolution satellite data such as from National Oceanic and Atmospheric Administration's (NOAA) Advanced Very High Resolution Radiometer (AVHRR) is practical and powerful. Vidal and Perrier (1990) were among the first users of NOAA-AVHRR images in irrigation management. The most extensive study of irrigation performance assessment was carried out by Alexandridis *et al.* (1999) using NOAA-AVHRR. They investigated the Indus river basin to identify the irrigated areas and assessed the performance of the irrigation systems. Boken *et al.* (2004) also demonstrated the potential of NOAA-AVHRR for estimating irrigated areas of three states of the USA. Thenkabail *et al.* (2005) used Moderate Resolution Imaging Spectroradiometer (MODIS) time series to generate land-use/land-cover (LULC) and an irrigated area mapping exercise for Ganges and Indus River basins in the Indian subcontinent. This study explains all the preprocessing operations and the methods required to handle time-series data sets for irrigated area mapping. Kamthonkiat *et al.* (2005) described a technique called peak detector algorithm to discriminate between rain-fed and irrigated rice crops in Thailand. This paper used a three-year time series of Satellite Pour l'Observation de la Terre vegetation (SPOT VGT) normalized difference vegetation index (NDVI) to identify cropping intensity. Satakmoto *et al.* (2006) worked on the Mekong and Bassac River basins to map the spatiotemporal distribution of rice cropping systems using MODIS. Biggs *et al.* (2006) used MODIS time series combined with ground truth data, agricultural census data and Landsat thematic mapper (TM) data to map surface water irrigation, groundwater irrigation and rain-fed ecosystems of the Krishna river basin in the southern Indian peninsula. Biggs *et al.* (2006) have stressed the importance of NDVI time series to identify and separate different types of irrigation including double-cropping systems, continuous irrigation, irrigated areas with low vegetation vigor and minor and groundwater irrigation. Xiao *et al.* (2006) mapped rice growing regions in the South and Southeast Asia using multi-temporal MODIS data. Thenkabail *et al.* (2006, 2009a, and 2009b) used time composites of NOAA AVHRR (10 km spatial resolution, 10-day composites) along with SPOT vegetation (1 km) and other data sets to derive irrigated areas for the entire world.

The above literature has consistently reported that single date fine-resolution imagery, acquired at critical growth stages, is sufficient to identify irrigation; multi-date time series are needed to distinguish difference between irrigated crop types and derive irrigation intensity (Thiruvengadachari, 1981; Rundquist *et al.*, 1989; Thenkabail *et al.*, 2005 and 2006). Furthermore, time series are absolutely critical for global studies where finer-resolution imagery will be extremely resource-intensive and bring many challenges in data handling. The methods applied for mapping irrigated areas at different scales ranging from field level to global scale are well established and validated (Thiruvengadachari, 1981; Boken *et al.*, 2004; Thenkabail *et al.*, 2006, 2009a, and 2009b). But there is no single method that can be applied to all the studies. Although single-date fine-spatial-resolution satellite data help to precisely identify the irrigated areas including minor and informal irrigation they fail to derive intensity of irrigation and cropping calendar of the crop identified. Time-series course-spatial-resolution data can derive intensity of irrigation and cropping calendar of all the crops under irrigation, but acquiring coarse-spatial-resolution data has its own advantages, such as availability of cloud-free, time series that can be downloaded for free and processed for near-cloud-free status using techniques like monthly maximum value composites (MVCs) from original daily data. Hence, to precisely identify the irrigated areas and also to derive irrigation intensity and a cropping calendar, there is a need to develop a methodology to integrate the use of both the fine-spatial and coarse-spatial-resolution data sets (Thenkabail *et al.*, 2006, 2009a, and 2009b). So, there is a need to bridge the gap between the use of fine-resolution-satellite data and the use of coarse-resolution-satellite data and to modify the existing methodology to derive irrigated areas using fine-resolution satellite data.

It is also obvious that precise estimates of irrigated areas are required to determine a reasonably accurate quantity of water use from irrigated agriculture. This is possible only if we can eliminate the discrepancy that exists in area estimates at various scales and resolutions. The goal of this study was to determine irrigated areas in a region using data from various resolutions or scales. More specifically, we will establish the relationships that exist in determining irrigated areas at various resolutions: AVHRR 10,000 m, MODIS 500 m, MODIS 250 m, and Landsat 30 m. The study was conducted in the Krishna River basin (India), the third largest river basin in India, where irrigation types vary from very large-scale surface water to fragmented groundwater. The climate and elevation also vary widely across the Krishna basin making it an ideal study area for this study. In general, since the fragmented minor irrigation is better mapped using finer-spatial-resolution data, the hypothesis "the finer the spatial resolution of the sensor data used, greater is the irrigated area derived" is tested in this study.

Methods

Study Area

The study area is the Krishna river basin (Figure 1) in India. This basin has various kinds of irrigation, such as major surface water, minor fragmented irrigation from groundwater, small reservoirs, and tanks. Rainfall varies from a very high 2,200 mm in the Western Ghats to 1,100 mm in the delta, to less than 500 mm in most of the middle basins which have a semiarid climate. The elevation also varies from about 1,400 m to a few meters in the delta. The climate is semiarid in the central part of the basin, sub-humid in the eastern delta, and sub humid-to-humid in the Western Ghats (Biggs *et al.*, 2006). The major cropping season is kharif which

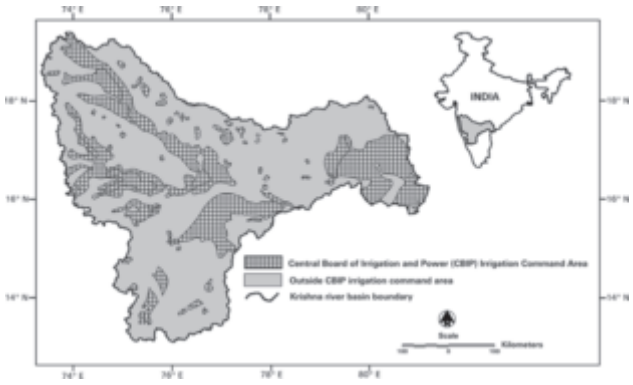

Figure 1. Study area: the Krishna River basin, India. The study was conducted in a very large river basin (258,922 km^2) that has large tracks of major and medium irrigated areas (hatched areas as per Central Board of Irrigation and Power (CBIP, 1994) and equally important fragmented informal irrigation from groundwater, small reservoirs and tanks, mostly outside the hatched areas).

extends from June to September followed by rabi (December to March). Land is left fallow in summer. These characteristics make the Krishna basin an ideal study site to investigate irrigated areas from various resolutions.

Study Approach

The primary objective of this study is to understand the issue of resolution in mapping irrigated areas. To do so, irrigated areas are mapped at 10,000 m, 500 m, 250 m, and 30 m (see Table 1). These maps are produced by more or less similar methodologies, so that the comparison of the areas derived is meaningful. All the data sets were generated for the nominal year of 2000.

Methodology for Mapping Irrigated Areas at Various Resolutions

A consistent set of methods and protocols were espoused and adopted for mapping irrigated areas at various resolutions. The process for each resolution involved the following steps:

- Data set identification including secondary data.
- Image normalization and synthesis including mosaicing and georectification.
- Megafile creation.
- Image masking and segmentation.
- Image classification and class spectra generation.
- Class identification and labeling process and protocols.
- Production of irrigated area maps.
- Area calculations, including sub-pixel area calculations for coarser-resolution-imagery.

In this paper, we discuss these methods and techniques to map irrigated areas using Landsat 30 m spatial resolution (Figure 2). Methods and protocols used for mapping irrigated areas using coarser-resolution data such as AVHRR (see Thenkabail *et al.*, 2006 and 2007a), and MODIS (Thenkabail *et al.*, 2005; Biggs *et al.*, 2006; Dheeravath *et al.*, 2009), follow similar approaches as for 30 m with certain inevitable distinctions, such as the use of time series, and calculation of irrigated areas based on sub-pixel areas (SPAs) (Thenkabail *et al.*, 2007b).

Data Sets used for Mapping Irrigated Areas at 30 m

The 30 m Landsat irrigated area map of the Krishna basin was developed based on the following data sets:

Landsat ETM+ Data

Twenty three Landsat ETM+ tiles were downloaded from the University of Maryland, Global Land Cover facility website (**http://glcf.umiacs.umd.edu/index.shtml**). All the images are from the nominal year 2000. All of them except one tile coincide with the main cropping season. One image over the central part of the basin, coinciding with the non-cropping season was classified and dealt with separately. All the Landsat ETM+ tiles were converted into reflectance to normalize the multi-date effect (Markham and Barker, 1986; Thenkabail *et al.*, 2004) using a model developed in ERDAS Imagine® (ERDAS, 2007).

Secondary Data Sets

Other than Landsat ETM+ tiles, the following secondary data sets were also used:

1. SRTM 90 m Elevation Data: The Shuttle Radar Topography Mission (SRTM) obtained elevation data on a near-global scale to generate the most complete high-resolution digital topographic database of the Earth (Farr and Kobrick, 2000; Rabus *et al.*, 2003; Rodriguez *et al.*, 2005; Farr *et al.*, 2007). Since the topography of the river basin under investigation is highly diverse, the SRTM elevation data set is useful in separating irrigated areas within the command areas and deltas with low elevations and high elevated areas with forest vegetation. The SRTM data (90 m resampled to 30 m) were also used to perform image segmentation based on elevation values in the basin.
2. MODIS 500 m Data Set: The MODIS 500 m monthly maximum composite data set is derived from the four 8-day composites of each month during 2001. These data are then resampled to 30 m and used in this study by integrating them with the Landsat data. The time series MODIS data help generate the cropping calendar for the classes identified from the Landsat ETM+ satellite data and help in the process of class identification and labeling.

TABLE 1. RESOLUTIONS USED IN MAPPING IRRIGATED AREAS. FOUR DISTINCT SPATIAL RESOLUTIONS INVOLVING AVHRR PATHFINDER, TERRA MODIS AND LANDSAT ETM+ WERE USED IN MAPPING IRRIGATED AREAS.

Serial no.	Resolution (meters)	Satellite	Sensor	Data type	Dates acquired	Frequency
1	10,000	NOAA	AVHRR	2 band reflectance; 2 band thermal, and NDVI	1998–1999	Monthly maximum value composite
2	500	TERRA	MODIS	7-band reflectance and NDVI	2001–2003	Monthly maximum value composite
3	250	TERRA	MODIS	2-band reflectance and NDVI	2005–2006	Monthly maximum value composite
4	30	LANDSAT	ETM+	6-band reflectance and NDVI	1999–2001	Single date, 6 nonthermal bands

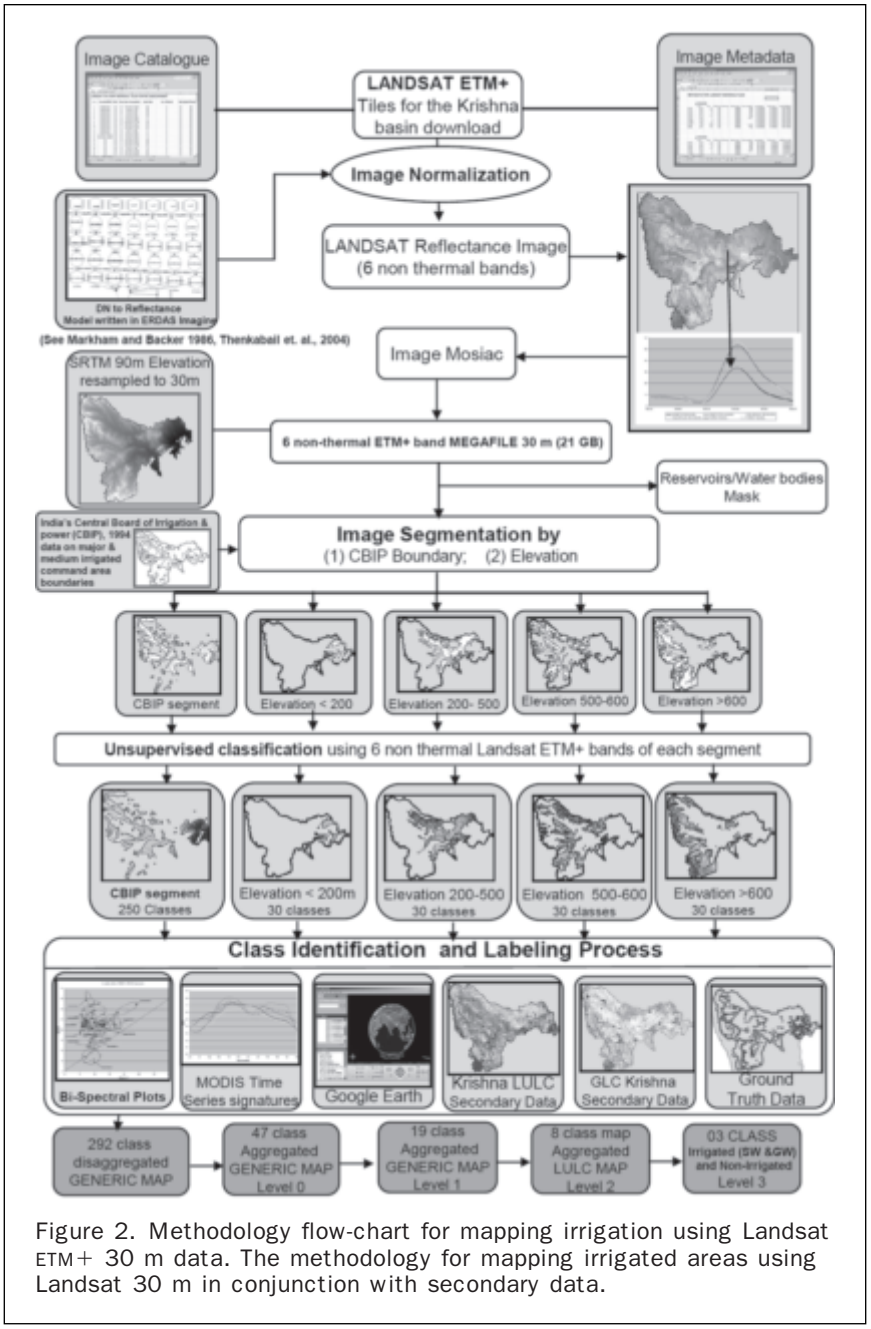

Figure 2. Methodology flow-chart for mapping irrigation using Landsat ETM+ 30 m data. The methodology for mapping irrigated areas using Landsat 30 m in conjunction with secondary data.

Methodology of Mapping Irrigated Areas at 30 m

An overview of the comprehensive methodology for mapping irrigated areas using Landsat ETM+ 30 m data is presented in Figure 2. The methodology consisted of the following steps:

Image Normalization

The Landsat images were converted into at-satellite reflectance using a reflectance model built in ERDAS Imagine® during this project based on the equations and algorithms presented in Markham and Barker (1986) and Thenkabail *et al.*, (2004). The digital number images were first converted to radiance and then to reflectance using the equations given in Markham and Baker, 1986 and Thenkabail *et al.*, 2004. The metadata needed for normalization are available in the header files.

Megafile Creation

A megafile consisting of the six non-thermal bands from each of 23 Landsat ETM+ tiles covering the entire Krishna basin was composed (see Thenkabail *et al.*, 2006, 2009a, and 2009b) for each segment (Figure 2).

Image Segmentation

The megafile was divided into six distinct zones (see Figure 2) based on (a) major irrigation command area zone using India's Central Board of Irrigation and Power (CBIP) command area map, (b) four SRTM-derived elevation zones, and (c) a zone of reservoirs, tanks, and other water bodies. The idea behind the segmentation process is to focus more on the segments having higher amounts of informal and fragmented irrigation classes such as the CBIP command areas. Such segments would be classified into more numbers of classes than the others for

better delineation of different irrigated classes using the protocols presented in Figure 2.

A segment based on the CBIP (1994) boundaries was used to demarcate the command areas irrigated by major and medium surface water reservoirs. The rest of the basin was segmented into four elevation zones as (a) less than 200 m, (b) 200 to 400 m, (c) 400 to 600 m, and (d) greater than 600 m. The SRTM data were used as the source of elevation. A simple model was built to slice the Landsat data into these four categories based on SRTM elevations. A mask was generated based on the simple threshold of mid-infrared ETM+ band 5 data (reflectance of 4 or less) and/or NDVI data (NDVI value 0.1 or less). This mask was used to extract water bodies from the Landsat data that were later eliminated from the classification process.

Class Spectra Generation

Each segment is then classified using unsupervised ISOCLASS clustering K-means classification (Tou and Gonzalez, 1974). The number of classes varied from 30 to 250 based on the areas covered by the segment and complexity of landscape. For example, the segment with elevation <200 m was mostly in delta areas, and 30 initial classes will be sufficient to determine distinct irrigation types. Since the CBIP segment covered large areas with complex irrigated and non-irrigated lands, it was classified into 250 classes.

Class Identification and Labeling Process

The class identification and labeling process involve the use of the following datasets (Figure 2):

1. Bispectral plots which represent every unsupervised class in two-dimensional feature space (2-d FS) plotted on red band versus near-infrared band. The mean values of band 3 (red) and band 4 (NIR) for each class were plotted and bispectral plots were derived (see Thenkabail *et al.*, 2005). From these plots, the mean NDVI values of the classes were grouped into different clusters based on their spatial location. Each such cluster contains classes with more or less identical LULC. Then, each class within a cluster was individually subjected to a protocol of class identification process described in detail by Thenkabail *et al.* (2005).
2. NDVI time-series plots which provide time-series "signatures" in terms of NDVI variations in a regular time interval (e.g., month by month).
3. Groundtruth Data Set: A total of 826 groundtruth points collected during several groundtruth missions by the International Water Management Institute (IWMI) (see **www.iwmidsp.org**) and 12 points from the degree confluence project (see **www.confluence.org**) were used for (a) class identification and labeling process, and (b) accuracy assessments.
4. Google Earth® Data Set: Since Google Earth® provides very high-resolution images from 30 m to sub-meter resolution for free and accessible through the web, this data set was also used for class identification and verification, especially to ascertain whether a class is irrigated or rain-fed croplands. Though Google Earth® does not guarantee pin point accuracy, the zoom-in views of high-resolution imagery were used to identify the presence of any irrigation structures (e.g., canals, irrigation channels, open wells). It was observed from the digital globe option on Google Earth® that most of the high-resolution imageries were acquired after the year 2000 and on average, Google Earth® high resolution imagery are one to three years old (Google Earth® Help). When definitive answers were not available (e.g., absence of irrigation structures) we did not use that particular Google Earth® data point in the analysis. Google Earth® high-resolution imagery, when used along with other distinct datasets, provides supplemental supportive results.
5. MODIS Time Series: Since the Landsat ETM+ images represent a single day scenario during the cropping season, MODIS time series (500 m resampled to 30 m) were used to derive the seasonal variations for the same pixel, thus deriving the cropping intensity for each pixel. The classified map is overlaid on the MODIS to derive the statistics. This information is used to build the time-series curves for the irrigated pixels. The cropping calendar sequence of the crop is derived from these time-series curves as explained by Thenkabail *et al.* (2005).
6. Other Secondary Data: Biggs *et al.* (2006) used MODIS 500 m data sets for 2002 to classify the irrigated areas within the Krishna river basin and produced a nine class irrigated and an LULC map for this basin. This was also used to cross-check the classes identified and labeled. The global LULC map produced by the Global Land Cover 2000 (GLC2000) for the entire world by an international partnership of 30 research groups was coordinated by the European Commission's Joint Research Centre (Bartholome and Belward, 2005). A subset of the GLC2000 for the Krishna River basin is used. This is a generic 45 class LULC map derived using SPOT VEGETATION at 1,000 m resolution. Classes 33 and 34 of this map correspond to irrigated areas (Agarwal *et al.*, 2003). These classes were also used in the class verification process.

The confidence of the class identified is increased as a result of multiple comparisons. First, the class is identified based on ground truth data, very high-resolution zoom in views of Google Earth® imagery, bispectral plots, and time-series NDVI plots. Second, when the identified class matches the majority of the secondary data, then the class is labeled and treated as resolved. Third, if the class is not definitively identified in the majority of these data sets, then it is sent back for the identification process again. Fourth, all the segments are classified using similar methodologies. In all the segments, each class is subjected to the entire class identification and labeling protocol.

A generic map containing 292 classes was generated by combining classes from all the five segments extracted from Landsat 30 m data. As the generic map contains classes from all the segments, it may contain classes with the same name. Similar classes with identical crop types and cropping intensities are merged to make a series of maps. Finally, a 19 class map with 13 distinct irrigated area classes and six other LULC classes were generated. However, in order to make inter-comparison of irrigated classes derived from MODIS and AVHRR, all distinct irrigated and non-irrigated classes were aggregated to three merged classes: (a) surface water irrigated, (b) ground water/conjunctive use irrigated, and (c) non-irrigated.

The methods for irrigated area mapping at coarser resolution (MODIS 250 m, 500 m, and AVHRR 10,000 m) follow the same approach as described above for Landsat 30 m with some differences in the megafile data-cube (MFDC) compositions (Thenkabail *et al.*, 2006, 2009a, and 2009b) and adoption of spectral matching techniques to analyze time-series images (Thenkabail *et al.*, 2007a) to produce aggregated two class irrigated and a non-irrigated class maps. Also, the finer resolutions provide full pixels areas (FPAs) which represent actual areas whereas in coarser resolution the FPAs are multiplied by irrigated area fractions (IAFs) to obtain actual areas.

Estimation of Irrigated Areas at Various Resolutions

Once the irrigated areas are mapped, the challenge is to determine precise areas. For finer resolutions (e.g., Landsat 30 m) the full pixel areas (FPAs) constitute actual areas. However, in coarser resolution (e.g., AVHRR, MODIS) sub-pixel areas (SPAs) will constitute actual areas. Hence, determining precise SPAs is a must when coarser resolution imagery is used.

The coarser the resolution of the pixel the greater the mix of land-cover and types within a pixel. So, it is appropriate to determine irrigated areas based on SPA estimation techniques (Thenkabail *et al.*, 2007b).

Sub-pixel Area (SPA) Calculation Methods

The SPAs are determined by multiplying FPAs with IAFs as shown in Equation 1.

$$SPA = FPA * IAF \quad (1)$$

where SPA is the sub-pixel area, FPA is the full pixel area (FPA), and IAF is the irrigated area fraction of the pixel.

The precision of irrigated area estimates depends on precise estimate of IAFs, which were determined using three distinct methods. These methods were: (a) IAF by Google Earth® very high-resolution "zoom in views" (IAF-GEE), (b) IAF by high-resolution imagery (IAF-HRI), and (c) IAF by sub-pixel decomposition technique (IAF-SPDT). As these methods are described in detail in a recently published paper by Thenkabail *et al.* (2007b) they will not be discussed here. The mean IAF used in this study is shown in Table 2.

Accuracy Assessment

Accuracy assessment was performed on three classes: surface water irrigated, ground water/conjunctive use irrigated, and non irrigated classes in order to compare a similar classes mapped using Landsat ETM+, MODIS 500m, MODIS 250m, and AVHRR 10km. Based on the theoretical description given by Congalton and Green (1999) Equations 2, 3, and 4 were used for the estimation of accuracies and errors. Two distinctly different and independent data sets as well as pooled data from the two sources were used to determine robust accuracies, using Equations 2, 3, and 4. These three data sets were: (a) Google Earth® data (GED), (b) Ground truth data (GTD), and (c) a combination of GED and GTD.

$$Accuracy\_of\_irrigated\_class = \frac{Groundtruthed\_irrigated\_points\_classificed\_as\_irrigated}{Tot\_number\_of\_groundtruthed\_points\_of\_rrigated\_class} \times 100 \quad (2)$$

$$Errors\_of\_commission = \frac{Non\_Irrigated\_groundtruth\_points\_classified\_as\_irrigated}{Tot\_number\_of\_nonirrigated\_groundtruth\_points} \times 100 \quad (3)$$

$$Errors\_of\_omission = \frac{Irrigated\_groundtruth\_points\_falling\_on\_nonirrigatedundclass}{Tot\_number\_of\_groundtruth\_points\_of\_irrigated\_area\_class} \times 100 \quad (4)$$

A total of 621 data points were used in the pooled datasets for accuracy assessments. The GED points were purely random and consisted of data obtained from 130 locations. There were 491 GTD points gathered during field campaigns. These data points were spatially well distributed and were used for accuracy assessments of three classes consistently generated from four spatial resolutions: 10,000 m, 500 m, 250 m, and 30 m data sets.

Results and Discussion

We will present, first, the results of irrigated areas at various resolutions and, second, the accuracies and errors at which these were mapped. Third, we will enumerate the ability to map irrigated area sources at various resolutions and finally, establish the relationships between resolutions in mapping irrigated areas.

Resolution and Irrigated Areas

The study reported irrigated areas derived from four distinct resolutions: 10,000 m, 500 m, 250 m, and 30 m based on AVHRR, MODIS, and Landsat ETM+ data (see Table 3 and Figures 3 and 4). The areas for the coarser resolutions were computed based on IAFs as reported in Table 2. Figure 4 shows the spatial distribution of the irrigated areas at various resolutions, and Table 3 summarizes their areas. The accuracies and errors of omission and commission for the irrigated areas at various resolutions were established and shown in Table 4.

TABLE 2. IRRIGATED AREA FRACTIONS (IAFS) AT VARIOUS RESOLUTIONS: THE IAFS AT 10,000 M, 500 M, 250 M AND 30 M FOR SURFACE WATER AND GROUNDWATER IRRIGATION SOURCES

Source of irrigation	LANDSAT 30 m	MODIS 250 m	MODIS 500 m	AVHRR 10,000 m
Surface water irrigation	1.000	0.79	0.72	0.67
Groundwater irrigation	1.000	0.72	0.59	0.61
Irrigation as a whole	1.000	0.75	0.65	0.64

The results showed that the irrigated areas increased with decrease in spatial resolution (Figure 3; Table 3). From the Landsat 30 m resolution data, the irrigated areas were 9.36 million hectares (Mha). From the MODIS 250 m data, the irrigated area was 95 percent of the Landsat 30 m derived irrigated areas (Table 3). This was further reduced to 92 percent of Landsat 30 m for MODIS 500 m resolution, and to 86 percent of Landsat 30 m for AVHRR Pathfinder 10,000 m (Figure 3 and Table 3). If the areas were calculated considering the FPAs as actual areas, then in such a situation, the coarser resolution will provide areas higher than finer resolution. But coarser resolution FPAs, typically constitute more than one land-cover category within a pixel, and hence calculating areas for any one land-cover category (e.g., irrigated areas) lead to overestimation of areas which can be misleading. The coarser the resolution of the pixel, the greater is the uncertainty in accurate area estimation.

The fragmented minor or informal irrigation (e.g., groundwater, small reservoirs, and tanks) means scattered areas surrounded by heterogeneous non-irrigated landscapes. Figure 5 shows the location of hundreds of small tanks that form an important component of informal irrigation throughout the Krishna basin. An overwhelming proportion of these fragments are captured at Landsat 30 m resolution. At coarser resolutions, these are captured as sub-pixel compositions. When the density of fragmented irrigation is high, the IAF will be high and vice-versa. However, when the density is poor, the pixel may be mapped as non-irrigated. It is

TABLE 3. RESOLUTIONS AND AREAS: THE SURFACE WATER AND GROUNDWATER IRRIGATED AREAS OF THE KRISHNA RIVER BASIN AT FOUR DISTINCT RESOLUTIONS: 10,000 M, 500 M, 250 M AND 30 M

		Source of irrigation						
		Surface water		Groundwater/ Conjunctive use		Total		
Serial no.	Resolution (meters)	Area (ha)	% TIA*	Area (ha)	% TlA*	TIA* (ha)	% to basin area**	% decrease w. r. t 30m
1	10,000	1,935,325	24	6,153,257	76	8,088,581	31	86
2	500	3,771,233	43	4,919,624	57	8,690,847	34	93
3	250	3,860,736	43	5,063,084	57	8,923,820	34	95
4	30	3,894,781	42	5,461,380	58	9,356,160	36	100

* TIA is Total irrigated area. ** The total basin area is 25.89 Mha.

possible to underestimate or overestimate the SPAs in coarser-resolution imagery depending on how accurately IAFs are determined (Thenkabail *et al.*, 2007b).

Accuracies and Errors in Mapping Irrigated Areas at Different Resolutions

The accuracies and errors (Table 4) in mapping irrigated areas were established for three classes (surface water irrigated, ground water/conjunctive use irrigated, and non-irrigated) generated at four spatial resolutions: 10,000 m, 500 m, 250 m, and 30 m. These accuracies and errors (Table 4) were established using 621 pooled data points as well as 130 GED points and 490 GTD points. Landsat 30 m data provided the best accuracies (84 percent) and the least errors of omission (16 percent) and commission (20 percent) when pooled GED and GTD points were used (Table 4). These are highly acceptable results. Accuracies were more or less in the same range for MODIS 250 and 500 m data (77 to 79 percent) but the errors of omission (21 to 23 percent) and commission (28 to 32 percent) were higher. However, it was interesting to see that MODIS 500 m data provided slightly better accuracy (by 2 percent) when compared to the MODIS 250 product. This may be attributed to the presence of more spectral bands in the MODIS 500 m data set. The AVHRR accuracies were significantly lower (63 percent), but the errors of omission (37 percent) and commission (25 percent) were nearly similar (Table 4). It must, however, be noted that most of the errors were as a result of inter-mixing between surface water irrigated versus ground water/conjunctive use irrigated. So, one can expect relatively higher accuracies (and lower errors) if the test was conducted only for irrigated areas (by combining surface and ground water/conjunctive use irrigated classes).

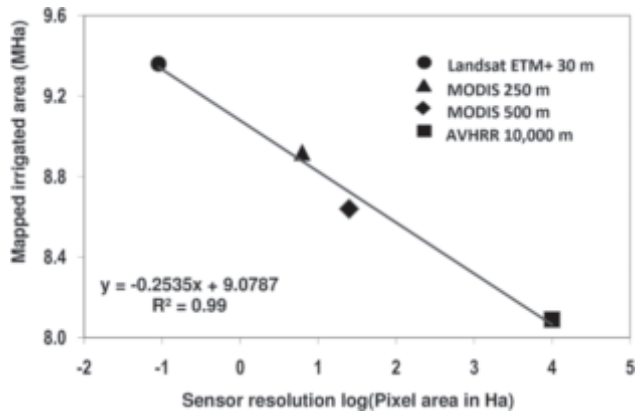

Figure 3. Implication of resolution on areas. The irrigated areas (in million hectares) mapped using (a) NOAA AVHRR 0.1 degree (10,000 m), (b) MODIS Terra visible and NIR bands (500m), (c) MODIS Terra red and NIR bands (250 m), and (d) Landsat ETM+ visible and NIR bands (30 m) plotted against the log (pixel area in Ha) of each sensor.

Sources of Irrigation as Determined at Various Resolutions

The irrigated areas based on the two main sources of irrigation were established at all resolutions (Table 3). The two main sources of irrigation were (a) major irrigation (areas irrigated from major and medium surface water reservoirs), and (b) minor irrigation (areas irrigated from groundwater, small reservoirs and tanks).

First, the estimates derived using Landsat 30 m show that there is a total irrigated area (TIA) of 9.36 Mha within the basin. Out of this, 3.9 Mha (42 percent) of area is irrigated through major sources (surface water) and 5.5 Mha (58 percent) through minor sources (groundwater or conjunctive use) (Table 3). Second, the trends of the irrigated areas from the two sources using MODIS 250 m and MODIS 500 m remained similar to the trend of Landsat 30 m (Table 3). The irrigated area estimates derived using MODIS 250 m showed that TIA within the basin was 8.9 Mha. Out of this 43 percent was irrigated by major sources and 57 percent by minor sources. The irrigated area estimates derived using MODIS 500 m show that TIA within the basin was 8.7 Mha. Out of this, 43 percent was irrigated by major sources and 57 percent by minor sources. Third, the irrigated area estimates derived using AVHRR 10,000 m show that TIA within the basin was 8.1 Mha. Out of this, only 22 percent was irrigated by major sources while 78 percent was irrigated by minor sources. This clearly indicates that at the very coarse resolution of 10,000 m, it is not possible to accurately distinguish between the major and minor sources of irrigated areas.

The spatial distribution of irrigated areas at various resolutions are presented in Figure 4. It is clear that fragmented irrigated areas are picked up with greater precision at finer resolution. Overall, the two MODIS resolutions provided nearly similar estimates of major and minor irrigations (Table 3). However, seven-band MODIS 500 m data showed slightly higher accuracy than the higher spatial resolution, two-band MODIS 250 m data set. The AVHRR resolution is too coarse to distinguish between the major and minor irrigation. Landsat 30 m does the best in differentiating major and minor irrigation.

The Krishna basin is considered a hydrologically closing basin. The outflow of water to the ocean is insignificant during normal rainfall years. Generally, it is thought that the increase in the number of irrigation projects and uncon-

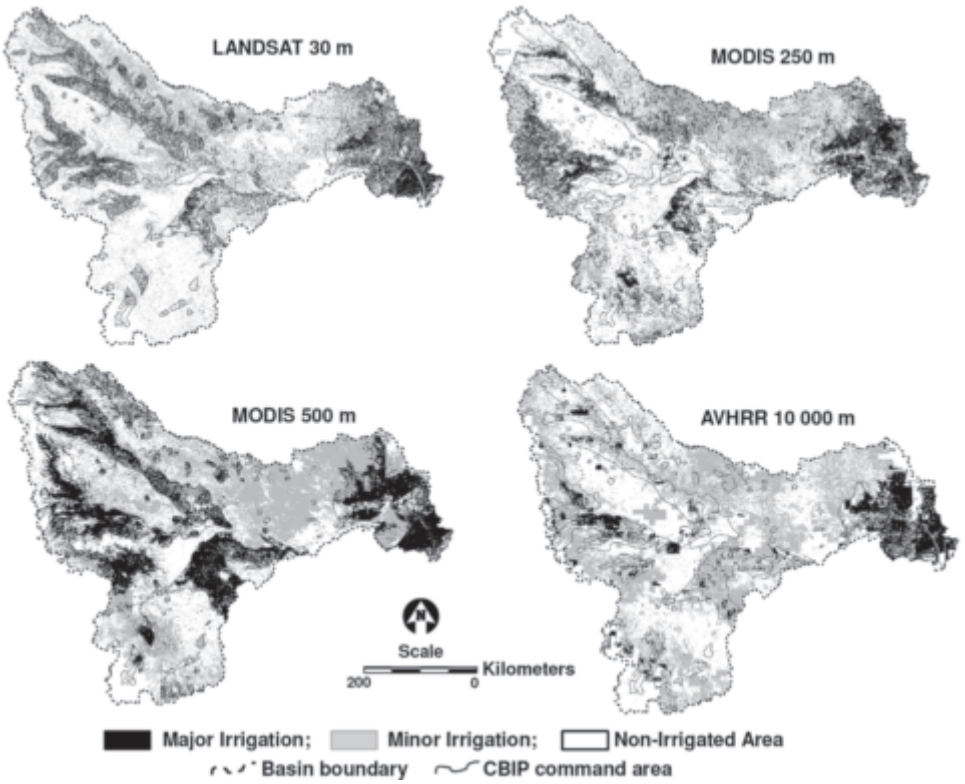

Figure 4. Spatial distribution of irrigated areas at various resolutions. At coarser resolution of AVHRR and MODIS, areas were determined based on sub-pixel fractions. At Landsat resolution, they were based on actual pixel area. Major irrigation includes surface water irrigation; Minor Irrigation includes ground water and conjunctive irrigation use. Areas in white within the basin are non-irrigated.

TABLE 4. ACCURACY ASSESSMENT AT VARIOUS RESOLUTIONS FOR SURFACE WATER IRRIGATION, GROUND WATER IRRIGATION AND NON-IRRIGATED CLASSES DETERMINED USING THREE SOURCES OF DATA; ACCURACY ASSESSMENT FROM: (A) GOOGLE EARTH® DATA (B) GROUND TRUTH DATA, AND (C) GOOGLE EARTH® + GROUND TRUTH DATA.

		Accuracy (%) using			Errors of Omissions (%)			Errors of Commission (%)		
S. No	Resolution (meters)	GED*	GTD#	GED + GTD	GED*	GTD#	GED + GTD	GED*	GTD#	GED + GTD
Surface Water Irrigation Class:										
1	10000	62	64	63	38	36	37	34	23	25
2	500	65	82	79	35	18	21	46	30	32
3	250	74	78	77	26	22	23	32	27	28
4	30	82	84	84	18	16	16	26	18	20
Ground Water Irrigation Class:										
1	10 000	60	55	56	40	45	44	54	59	58
2	500	66	70	69	34	30	31	58	44	48
3	250	51	69	64	44	31	36	49	49	48
4	30	77	73	74	23	27	26	29	41	38
Non-Irrigation Class:										
1	10 000	59	69	66	41	31	34	31	31	31
2	500	48	62	59	52	38	41	15	15	15
3	250	75	64	67	25	56	33	25	17	19
4	30	82	75	76	18	34	24	7	12	11

* GED = Google Earth® Data (n = 130);
# GTD = Ground Truth Data (n = 491) collected during this project by the International Water Management Institute (IWMI) and sourced through degree confluence project (DCP)

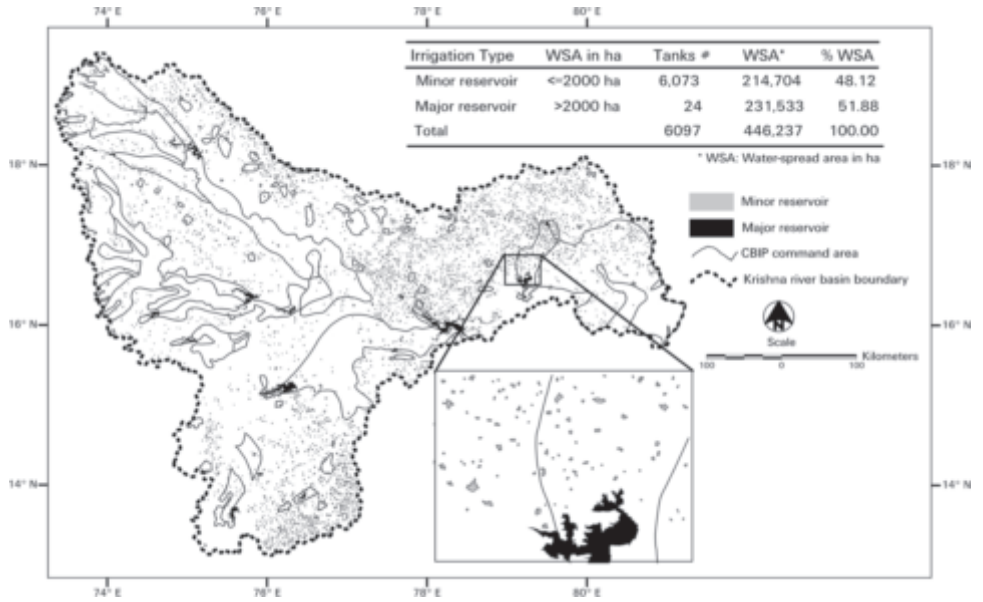

Figure 5. Distribution of major and minor irrigation in the Krishna River basin determined using Landsat ETM+. The outer boundaries of the major and medium irrigation command areas in the Krishna basin (Data: India's Central Board of Irrigation and Power, 1994) are shown in gray shade. These areas are classified separately to determine actual areas irrigated. The minor irrigation consists of areas irrigated by groundwater, small reservoirs and tanks, and are typically outside the command areas and are delineated using Landsat ETM+.

trolled groundwater abstraction in recent years have led to the basin closure (Venot *et al.*, 2007; Biggs *et al.*, 2007). In this study, 6,097 small tanks larger than about 5 ha water spread area were mapped by Landsat 30 m data (Figure 5; Table 5). The 24 major reservoirs are the main sources of the surface water irrigation within the basin. India's Central Board of Irrigation and Power (CBIP, 1994) has delineated the boundary of command areas for these major reservoirs (Figure 1). It is interesting to see from Figure 5 that, the most of the CBIP areas in the upper basin are relatively free from small tanks since large reservoirs are being used for irrigation. The contribution of these major reservoirs to the total irrigation is only 46 percent (Table 5). However in the lower basin, since the ground water table level is generally low, large numbers of small tanks are being used for irrigation purposes even within the CBIP areas. In the rest of the area, the reservoirs, small tanks (with water spread areas less than 2,000 ha but greater than 5 ha), and groundwater contribute up to 54 percent of the basin irrigated area; groundwater contributes 74 percent of this 54 percent area. Other remote sensing and GIS data sets such as Global Land Cover map (GLC2000) (Bartholome and Belward, 2005), MODIS LULC map (Biggs *et al.*, 2006), and Global Lake and Wetland Data set (GLWD) (Lehner and Doll, 2004) were used to compare the number and the area covered by these water bodies within the Krishna River basin (see Table 6). The comparative results (Table 6) suggest that none of the existing secondary data could capture the small water bodies present within the

TABLE 5. AREAS FROM MAJOR AND MINOR IRRIGATION SOURCES DETERMINED USING LANDSAT ETM+ 30 M DATA; IRRIGATED AREAS FROM MAJOR AND MEDIUM IRRIGATION SOURCES (RESERVOIRS WITH >2,000 HA WATER-SPREAD AREA) VERSUS IRRIGATED AREAS FROM MINOR SOURCES (GROUNDWATER, SMALL RESERVOIRS AND TANKS)

				Total irrigated area (TIA)					
Size of reservoirs (ha)	No. of reservoirs	WSA* (ha)	Percent to the total WSA	SWI# (ha)	Irrigated (%)	GWI$ (ha)	Irrigated (%)	TIA (ha)	TIA (%)
A. Major and medium irrigation									
> 5,000	10	191,582	42.93	2,882,784	74	1,439,818	26	4,322,602	46
>2,000 and <=5,000	14	39,951	8.95						
B. Minor irrigation									
>1,000 and <=2,000	21	28,707	6.43						
>500 and <=1,000	18	11,218	2.52	1,011,997	26	4,021,562	74	5,033,559	54
>100 and <=500	295	55,720	12.49						
> 5 and <=100	5,739	119,059	26.68						
Total	6,097	446,237	100.00	3,894,781	100	5,461,380	100	9,356,160	100

* WSA = Water-spread area; # SWI = Surface water irrigation; $ GWI = Groundwater irrigation.

TABLE 6. COMPARISON OF WATER BODIES DERIVED FROM VARIOUS DATA SETS; NUMBER AND SURFACE AREA OF WATER BODIES AS DERIVED FROM REMOTE SENSING AND GIS DATA SETS

Serial No.	Data set	Reference	Number of water bodies	Surface area in ha
1	MODIS	Biggs *et al.*, 2006	1,174	252,577
2	GLWD	Lehner and Doll, 2004	1,022	368,971
3	GLC2000	Bartholome and Belward, 2005	90	387,358
4	Landsat	This study	6,097	446,237

study area. The reason for this is the coarse resolution of the data used to build the water bodies' data set. The difference in surface area between the Landsat-derived water bodies in this study and those of other reported studies (Table 6) was due to inadequate or non-accounting of small reservoirs, tanks, and groundwater irrigation in other studies which used coarser resolution imagery. Even at Landsat 30 m resolution, there are uncertainties since tanks with areas smaller than 5 ha are missing at this resolution as well. Also, seasonal tanks are missing here since the images are for single dates. These two factors possibly result in a significant number of missing tanks and hence irrigated areas. Biggs *et al.* (2007) reported that within the Krishna basin, there are nearly 66,000 tanks within Andhra Pradesh alone (eastern part of the Krishna basin). Shiva (1991) also claimed that small tanks are common in the Karnataka region (south-western region of the Krishna basin). These tanks spatially spread over the basin, tap the drainage flow of rainwater and act as temporary storage structures. Such tanks act as sources of irrigation (both surface water and conjunctive use) for several thousands of hectares of land. Also, these small tanks recharge the groundwater aquifers substantially, and the water is tapped elsewhere for irrigation purposes. Further investigation is required to study the impact of these enormous numbers of water bodies on the basin closure.

Relationships between the Resolutions in Determining Irrigated Areas

A general relationship between irrigated area mapped and the sensor resolution is shown in Figure 3. Further, relationships linking irrigated areas mapped at different resolutions were developed based on the data for 35 districts ($n = 35$) within the Krishna basin (Figure 6). These are the districts that fall fully within the basin. The irrigated areas from AVHRR 10,000 m, MODIS 500 m, and MODIS 250 m were derived by applying appropriate irrigated area fractions and compared with irrigated areas derived from 30 m. The relationships in computing irrigated areas between various resolutions were strong with an R^2 value between 0.74 and 0.95 (Figure 6). The higher R^2 values were for closer resolutions: 0.95 between 10,000 m and 500 m: 0.75 between 500 m and 250 m, and 0.85 between 250 m and 30 m. The results imply the possibilities of determining irrigated areas at other resolutions, if the area at any one resolution is known. However, the precise locations of irrigated areas improve only with finer-spatial-resolution data (Figure 4).

Precision in Mapping Irrigated Areas across Scales

Investigations were made with reference to the precise physical location of the irrigated pixels across the resolutions. First, to make pixel-by-pixel comparison possible, all the data sets were resampled to 30 m. To ascertain precision of mapping irrigated areas of each product under study and also to achieve pixel by pixel comparison, a model built in ERDAS Imagine® was used. Results indicate that AVHRR 10,000 m, MODIS 500 m, and 250 m products, had 87 percent, 90 percent, and 95 percent match, respectively, with the Landsat product for total irrigated area without reference to the location of the pixel, and showed 100 percent, 79 percent, and 58 percent match, respectively, with reference to the location of the pixel. The higher match with coarser resolution was due to the very large size of the pixel in coarser-resolution satellites. However, due to the sub-pixel compositions and irrigated area fractions (IAFs), coarser-resolution data had less area than finer-resolution data sets. Also, the coarser-resolution data sets did not have exact representation of irrigated areas as seen by satellite data with spatial resolution of 30 m. But it is interesting to note that the coarser-resolution satellites preserve the overall integrity and ability to identify irrigated areas as a whole.

A Discussion on the Effect of Resolution on Irrigated Areas

Ideally, the area under irrigation or any LULC type should be the same irrespective of being mapped by sensors with different resolutions. However, areas determined from sensors with different resolutions often do not match. Since a single pixel in a coarser-resolution satellite data contains information from more than one feature or land-use type, quantifying the area under each land-use type requires understanding of sub-pixel composition. However, when the irrigated area fractions for each pixel are accurately identified, then areas estimated should be similar irrespective of the resolutions of the sensors under study. Accurate calculation at coarser resolution depends on the accuracy of sub-pixel area computation that, in turn, is dependent on IAFs. The IAFs were computed in this study based on three methods (Thenkabail *et al.*, 2007b), and hence they are quite robust. Nevertheless, the accuracies can improve if we have a greater local knowledge of pixel dynamics through greater sampling of pixels during ground truthing. Since the finer-resolution satellites cover smaller areas, it is more likely that a single pixel covers more or less similar LULC class and allows fewer errors in the area estimations. Uncertainties in area calculations are always likely to be higher with coarser-resolution imagery. Strong relationships exist in areas between resolutions (Figure 6), but often there is a consistent under-estimation of areas in coarser resolution imagery.

Conclusions

This study developed relationships between four distinct spatial resolutions: (a) AVHRR 10,000 m, (b) MODIS 500 m, (c) MODIS 250 m, and (d) Landsat ETM+ 30 m in determining irrigated areas. The outcomes of the research were as follows.

1. **The finer the spatial resolution, greater was the irrigated area mapped**: The irrigated areas within the Krishna River basin (for the nominal year of 2000) derived using Landsat ETM+ 30 m was 9.4 Mha. In comparison, the area derived using (a) MODIS 250 m was 8.9 Mha, (b) MODIS 500 m was 8.6 Mha, and (c) AVHRR 10,000 m was 8.1 Mha. This clearly proved our hypotheses that the finer the spatial resolution, greater was the area mapped, demonstrating the ability of the finer resolution data in detecting fragmented irrigated areas better. This concept needs further investigation over different

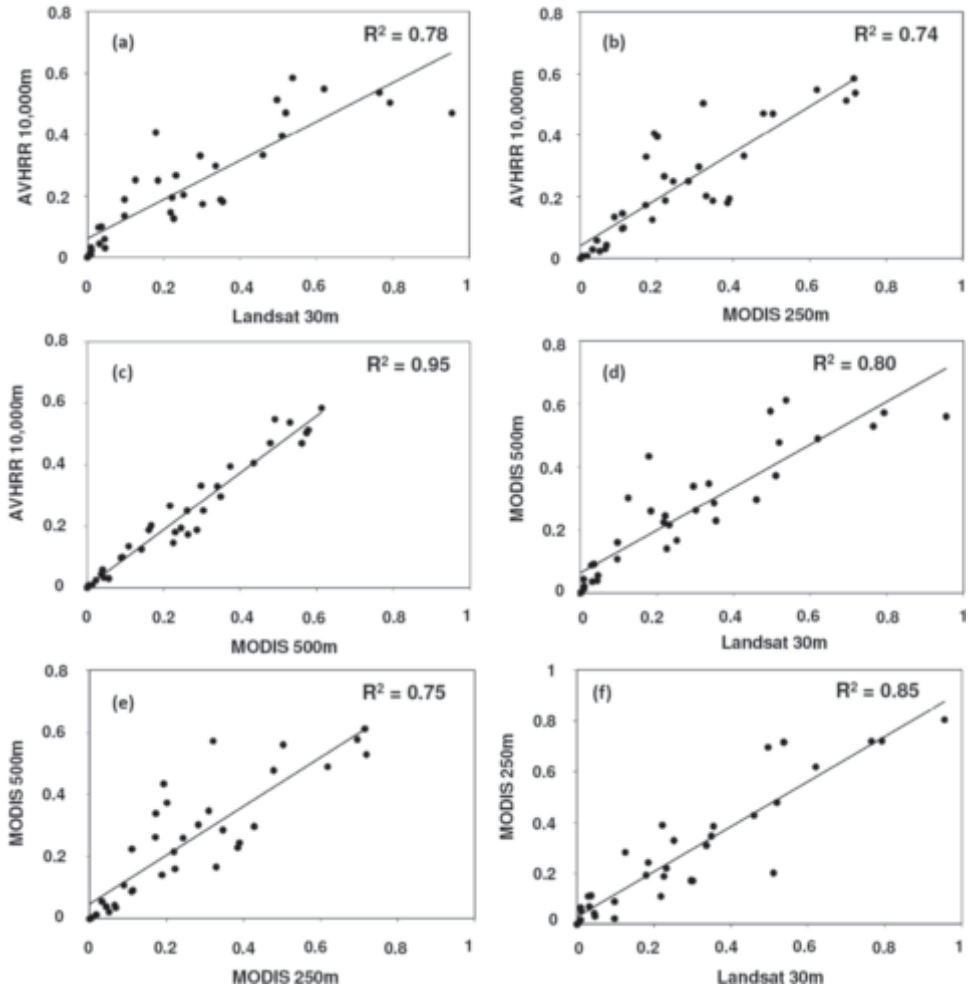

Figure 6. Relationships between irrigated areas (in Mha) determined at different resolutions for 35 districts within the Krishna basin. The R^2 values of areas determined between various resolutions varied between 0.74 and 0.95.

conditions having varying amounts of contiguous and fragmented irrigated areas. However, this hypothesis, in general, would be highly useful to make meaningful inferences and inter-comparisons of any area estimates derived using multi-resolution satellite data.

2. **Strengths of Landsat 30m data over coarser resolution data in detecting irrigated areas**: When compared to other coarser resolution satellite imagery, the Landsat 30 m data has two distinct strengths in mapping irrigated areas: (a) the ability to precisely determine the geographic location of the irrigated areas, and (b) to locate fragmented and minor irrigation sources such as small reservoirs, tanks, and ground water.
3. **Closer the two resolutions, closer were the irrigated areas estimated by them:** Comparison of irrigated areas estimated from all the four resolutions (AVHRR 10 km, MODIS 500 m, MODIS 250 m, and Landsat 30 m) revealed that the R^2 values for irrigated areas computed based on any two resolutions varied between 0.74 and 0.95, with better correlations between closer resolutions.
4. **Finer spatial resolution is critical for discerning crop types; however, spectral resolution critical to higher accuracies, not just the spatial resolution**: The accuracies in mapping irrigated areas varied between 63 and 84 percent with errors of omission not exceeding 37 percent and errors of commission not exceeding 32 percent. The high spectral resolution, MODIS 500 m data set yielded slightly higher classification accuracy when compared to the higher spatial resolution MODIS 250 m data. The finer resolutions, however, can discern crop types more accurately.
5. **Importance of irrigated area fractions (IAFs) in accurate determination of irrigated areas:** For the coarser-resolution satellite data, it was observed that the accuracies of irrigated area estimates are highly dependent on the accuracies of the irrigated area fractions used. Hence, accurate determination of IAFs is very critical to derive accurate estimates of the irrigated areas.

Acknowledgments

This study was supported by the International Water management Institute's (IWMI) core funding. We want to acknowledge the vision and support shown by Professor Frank Rijsberman, Program Director, Google (formerly Director General of IWMI). We thank three anonymous reviewers for their helpful comments and suggestions. The paper has not been internally reviewed by U.S. Geological Survey (USGS). Hence, the views expressed in the paper are not endorsed by USGS.

References

Abderrahman, W.A., and T.A. Bader, 1992. Remote sensing application to the management of agricultural drainage water in severely arid region: A case study, *Remote Sensing of Environment*, 42(3):239–246.

Agarwal, S., P.K. Joshi, Y. Shukla, and P.S. Roy, 2003. SPOT vegetation multi temporal data for classifying vegetation in south central Asia, *Current Science*, 84(11):1440–1448.

Alexandridis, T., S. Asi, and S. Ali, 1999. *Water Performance Indicators Using Satellite Imagery for the Fordwah Eastern Sadiqia (South) Irrigation and Drainage Project*, Report Number-87, International Water Management Institute, Lahore, Pakistan, 16 p.

Ambast, S.K., A.K. Keshari, and A.K. Gosain, 2002. Satellite remote sensing to support management of irrigation systems: Concepts and approaches, *Irrigation & Drainage*, 51:25–39.

Bartholome, E., and A.S. Belward, 2005, GLC2000: A new approach to global land cover mapping from earth observation data, *International Journal of Remote Sensing*, 26(9):1959–1977.

Bastiaanssen, W.G.M., D.J. Molden, S. Thiruvengadachari, A.A.M.F.R. Smit, L. Mutuwatte, and G. Jayasinghe, 1999. *Remote Sensing and Hydrologic Models for Performance Assessment in Sirsa Irrigation Circle, India,* Research Report 27, International Water Management Institute, Colombo, Sri Lanka.

Biggs, T., P.S. Thenkabail, M.K. Gumma, C.A. Scott, G.R. Parthasaradhi, and H.N. Turral, 2006. Irrigated area mapping in heterogeneous landscapes with MODIS time series, ground truth and census data, Krishna Basin, India, *International Journal of Remote Sensing*, 27(19):4245–4266.

Biggs, T.W., A. Gaur, C.A. Scott, P. Thenkabail, P.G. Rao, G.M. Krishna, S. Acharya, H. Turral, 2007. *Closing of the Krishna Basin: Irrigation, Streamflow Depletion and Macroscale Hydrology*, IWMI Research Report 111, *International Water Management Institute*, Colombo, Sri Lanka.

Boken, V.K., G. Hoogenboom, F.N. Kogan, J.E. Hook, D.L. Thomas, and K.A. Harrison, 2004. Potential of using NOAA-AVHRR data for estimating irrigated area to help solve an inter-state water dispute, *International Journal of Remote Sensing*, 25(12): 2277–2286.

CBIP (Central Board of Irrigation and Power), 1994. *Irrigation Atlas of India*, *Volume II,* Government Press, New Delhi.

Congalton, R.G., and K. Green, 1999. *Assessing the Accuracy of Remotely Sensed Data: Principles and Practices*, Lewis Publishers, Boca Raton, Florida, 137 p.

Dheeravath, V., P.S. Thenkabail, G. Chandrakantha, P. Noojipady, C.B. Biradar, H. Turral, M. Gumma, G.P.O. Reddy, and M. Velpuri, 2009. *Irrigated areas of India derived using MODIS 500m data for years 2001–2003*, ISPRS Journal of Photogrammetry and Remote Sensing, URL: *http://dx.doi.org/10.1016/j.isprsjprs.2009.08.004* (last date accessed: 20 October 2009).

Draeger, W.C., 1977. Monitoring irrigated land acreage using LANDSAT imagery: An application example, *ERIM Proceedings of the 11th* International Symposium on Remote Sensing of Environment, Volume 1, pp. 515–524 (SEE N78-14464 05-43).

Droogers, P., 2002. *Global Irrigated Area Mapping: Overview and Recommendations,* Working Paper 36, International Water Management Institute, Colombo, Sri Lanka.

ERDAS, 2007. *ERDAS Field Guide, Volume 1,* October 2007. URL: *http://gi.leica- geosystems.com/documents/pdf/FieldGuide_Vol1.pdf* (last date accessed: 10 September 2009).

Farr, T.G.,and M. Kobrick, 2000. Shuttle Radar Topography Mission produces a wealth of data, *EOS Transactions. AGU*, *81*,583–585.

Farr, T.G., P.A. Rosen, E. Caro, R. Crippen, R. Duren, S. Hensley, M. Kobrick, M. Paller, E. Rodriguez, L. Roth, D. Seal, S. Shaffer, J. Shimada, J. Umland, M. Werner, M. Oskin, D. Burbank, and D. Alsdorf, 2007. The Shuttle Radar Topography Mission, *Reviews of Geophysics*, 45, RG2004, doi:10.1029/2005RG000183.

Google Earth Help, 2009. URL: *http://groups.google.com/group/earth-data/browse_thread/thread/459aaf92464e9673#* (last date accessed: 10 September 2009).

Kamthonkiat, D., K. Honda, H. Turral, N.K. Tripathi, and V. Wuwongse, 2005. Discrimination of irrigated and rainfall rice in a tropical agricultural system using SPOT VEGETATION NDVI and rainfall data, *International Journal of Remote Sensing,* 26(12):2527–2547.

Keene, K.M., and C.D. Conley, 1980. Measurement of irrigated acreage in Western Kansas from LANDSAT images, *Environmental Geology, Earth and Environmental Science*, 3(2):107–116.

Lehner, B., and P. Döll, 2004. Development and validation of a global database of lakes, reservoirs and wetlands, *Journal of Hydrology*, 296/1–4:1–22.

Markham, B.L., and J.L. Barker, 1986. *Landsat MSS and TM Post-Calibration Dynamic Ranges, Exoatmospheric Reflectances and At-Satellite Temperatures*, Earth Observation Satellite Company, Lanham, Maryland, Landsat Technical Notes, 1, August.

Molden, D., 2007. *Water for Food, Water for Life, A Comprehensive Assessment of Water Management in Agriculture,* Earthscan, London.

Murthy, C.S., P.V. Raju, S. Jonna, K.A. Hakeem, and S. Thiruvengadachari, 1998. Satellite derived crop calendar for canal operation schedule in Bhadra project command area, India, *International Journal of Remote Sensing*, 19(15):2865–2876.

Ozdogan, M., C.E. Woodcock, and G.D. Salvucci, 2003. Monitoring changes in summer irrigated crop area in southeastern Turkey using remote sensing, *Proceedings of the 2003 IEEE International Geoscience and Remote Sensing Symposium, IGARSS*, 3(21–25):1570–1572.

Rabus, B., M. Eineder, A. Roth, and R. Bamler, 2003, The shuttle radar topography mission - A new class of digital elevation models acquired by spaceborne radar, *Photogrammetric Engineering & Remote Sensing*, 57(2):241–262.

Rodriguez, E., C.S. Morris, J.E. Belz, E.C. Chapin, J.M. Martin, W. Daffer, and S. Hensley, 2005, *An Assessment of the SRTM Topographic Products*, Technical Report JPL D-31639, Jet Propulsion Laboratory, Pasadena, California, 143 p.

Rundquist, D.C., H. Richardo, M.P. Carlson, and A. Cook, 1989. The Nebraska center-pivot inventory - An example of operational satellite remote sensing on a long-term basis, *Photogrammetric Engineering & Remote Sensing*, 55(5):587–590.

Sakthivadivel, R., S. Thiruvengadachari, U. Amerasinghe, W.G.M. Bastiaanssen, and D. Molden, 1999. *Performance Evaluation of the Bhakra Irrigation System, India, Using Remote Sensing and GIS Techniques*, Research Report 28, International Water Management Institute, Colombo, Sri Lanka.

Satakmoto, T., N.V. Nguyen, H. Ohno, N. Ishitsuka, and M. Yokozawa, 2006. Spatio-temporal distribution of rice phenology and cropping systems in the Mekong Delta with special reference to the seasonal water flow of the Mekong and Bassac Rivers, *Remote Sensing of Environment*, 100:1–16.

Shiva, V., 1991. Large dams and conflicts in the Krishna River basin, *Ecology and Politics of Survival, Conflicts over Natural Resources in India*, United Nations University Press, Tokyo.

Siebert, S., and J. Hoogeveen, 2006. Global mapping of irrigated areas by combining sub-national statistics and geo-spatial data on irrigation, *Proceedings of the Workshop on Global Irrigated Area Mapping*, International Water Management Institute, Colombo, 25.

Thenkabail, P.S., E.A. Enclona, and M.S. Ashton, 2004. Hyperion, IKONOS, ALI, ETM+ sensors in the study of African rainforests, *Remote Sensing of Environment,* 90:23–43.

Thenkabail, P.S., M. Schull, and H. Turral, 2005. Ganges and Indus river basin land use/landcover (LULC) and irrigated area mapping using continuous streams of MODIS data, *Remote Sensing of Environment,* 95:317–341.

Thenkabail, P.S., C.M. Biradar, H. Turral, P. Noojipady, Y.J. Li, J. Vithanage, V. Dheeravath, M. Velpuri, M. Schull, X. Cai, and R. Dutta, 2006. *An Irrigated Area Map of the World (1999) Derived from Remote Sensing, Research Report 105,* International Water Management Institute, Colombo, Sri Lanka.

Thenkabail, P.S., P. Gangadhara Rao, T. Biggs, M. Krishna, and H. Turral, 2007a. Spectral matching techniques to determine historical land use/land cover (LULC) and irrigated areas using time-series AVHRR Pathfinder datasets in the Krishna River basin, India, *Photogrammetric Engineering & Remote Sensing*, 73(9):1029–1040.

Thenkabail, P.S., C.M. Biradar, P. Noojipady, X. Cai, V. Dheeravath, Y.J. Li, M. Velpuri, M.K. Gumma, and S. Pandey, 2007b. Sub-pixel area calculation methods for estimating irrigated areas, *Sensors*, 7:2519–2538.

Thenkabail. P., G.J. Lyon, H. Turral, and C.M. Biradar, 2009a., *Remote Sensing of Global Croplands for Food Security*, CRC Press, Taylor and Francis Group, Boca Raton, London, New York, pp. 556.

Thenkabail, P.S., C.M. Biradar, P. Noojipady, V. Dheeravath, Y.J. Li, M. Velpuri, M. Gumma, G.P.O. Reddy, H. Turral, X.L. Cai, J. Vithanage, M. Schull, and R. Dutta, 2009b. Global irrigated area map (GIAM), derived from remote sensing, for the end of the last millennium, International Journal of Remote Sensing, 30(14):3679–3733.

Thiruvengadachari, S., 1981. Satellite sensing of irrigation pattern in semiarid areas: An Indian study, *Photogrammetric Engineering & Remote Sensing,* 47(12):1493–1499.

Thiruvengadachari, S., and R. Sakthivadivel, 1997. *Satellite Remote Sensing for Assessment of Irrigation System Performance: A Case Study in India,* Research Report 9, International Irrigation Management Institute, Colombo, Sri Lanka.

Tou, J.T., and R.C. Gonzalez, 1974. Pattern recognition principles, *Applied Mathematics and Computation* (R. Kalaba, editor), Addison-Wesley, Reading, Massachusetts.

Venot, J.P., H. Turral, M. Samad, and F. Molle, 2007. *Shifting Waterscapes: Explaining Basin Closure in the Lower Krishna Basin, South India,* IWMI Research Report 121, International Water Management Institute, Colombo, Sri Lanka.

Vidal, A., and A. Perrier, 1990. Irrigation monitoring by following the water balance from NOAA-AVHRR thermal infrared data, *IEEE Transactions on Geoscience and Remote Sensing,* 28:949–954.

Xiao, X., S. Boles, S. Frolking, C. Li, J.Y. Babu, W. Salas, and B. Moore, 2006. Mapping paddy rice agriculture in South and Southeast Asia using multi-temporal MODIS images, *Remote Sensing of Environment*, 100:95–113.

(Received 25 March 2008; accepted 13 January 2009; revised 24 March 2009)